Evidence of color coherence effects in W + jets events from $p\overline{p}$ collisions at $\sqrt{s} = 1.8$ TeV

B. Abbott, M. Abolins, V. Abramov, B.S. Acharya, I. Adam, D.L. Adams, M. Adams, S. Ahn, V. Akimov, G.A. Alves, et al.

HAL Id: in2p3-00003140

https://hal.in2p3.fr/in2p3-00003140

Submitted on 27 Oct 1999

Evidence of Color Coherence Effects in W+jets Events from $p\overline{p}$ Collisions at $\sqrt{s} = 1.8$ TeV

B. Abbott,[45] M. Abolins,[42] V. Abramov,[18] B.S. Acharya,[11] I. Adam,[44] D.L. Adams,[54]
M. Adams,[28] S. Ahn,[27] V. Akimov,[16] G.A. Alves,[2] N. Amos,[41] E.W. Anderson,[34]
M.M. Baarmand,[47] V.V. Babintsev,[18] L. Babukhadia,[20] A. Baden,[38] B. Baldin,[27]
S. Banerjee,[11] J. Bantly,[51] E. Barberis,[21] P. Baringer,[35] J.F. Bartlett,[27] A. Belyaev,[17]
S.B. Beri,[9] I. Bertram,[19] V.A. Bezzubov,[18] P.C. Bhat,[27] V. Bhatnagar,[9]
M. Bhattacharjee,[47] G. Blazey,[29] S. Blessing,[25] P. Bloom,[22] A. Boehnlein,[27] N.I. Bojko,[18]
F. Borcherding,[27] C. Boswell,[24] A. Brandt,[27] R. Breedon,[22] G. Briskin,[51] R. Brock,[42]
A. Bross,[27] D. Buchholz,[30] V.S. Burtovoi,[18] J.M. Butler,[39] W. Carvalho,[3] D. Casey,[42]
Z. Casilum,[47] H. Castilla-Valdez,[14] D. Chakraborty,[47] K.M. Chan,[46] S.V. Chekulaev,[18]
W. Chen,[47] D.K. Cho,[46] S. Choi,[13] S. Chopra,[25] B.C. Choudhary,[24] J.H. Christenson,[27]
M. Chung,[28] D. Claes,[43] A.R. Clark,[21] W.G. Cobau,[38] J. Cochran,[24] L. Coney,[32]
W.E. Cooper,[27] D. Coppage,[35] C. Cretsinger,[46] D. Cullen-Vidal,[51] M.A.C. Cummings,[29]
D. Cutts,[51] O.I. Dahl,[21] K. Davis,[20] K. De,[52] K. Del Signore,[41] M. Demarteau,[27]
D. Denisov,[27] S.P. Denisov,[18] H.T. Diehl,[27] M. Diesburg,[27] G. Di Loreto,[42] P. Draper,[52]
Y. Ducros,[8] L.V. Dudko,[17] S.R. Dugad,[11] A. Dyshkant,[18] D. Edmunds,[42] J. Ellison,[24]
V.D. Elvira,[47] R. Engelmann,[47] S. Eno,[38] G. Eppley,[54] P. Ermolov,[17] O.V. Eroshin,[18]
J. Estrada,[46] H. Evans,[44] V.N. Evdokimov,[18] T. Fahland,[23] M.K. Fatyga,[46] S. Feher,[27]
D. Fein,[20] T. Ferbel,[46] H.E. Fisk,[27] Y. Fisyak,[48] E. Flattum,[27] G.E. Forden,[20] M. Fortner,[29]
K.C. Frame,[42] S. Fuess,[27] E. Gallas,[27] A.N. Galyaev,[18] P. Gartung,[24] V. Gavrilov,[16]
T.L. Geld,[42] R.J. Genik II,[42] K. Genser,[27] C.E. Gerber,[27] Y. Gershtein,[51] B. Gibbard,[48]
G. Ginther,[46] B. Gobbi,[30] B. Gómez,[5] G. Gómez,[38] P.I. Goncharov,[18] J.L. González Solís,[14]
H. Gordon,[48] L.T. Goss,[53] K. Gounder,[24] A. Goussiou,[47] N. Graf,[48] P.D. Grannis,[47]
D.R. Green,[27] J.A. Green,[34] H. Greenlee,[27] S. Grinstein,[1] P. Grudberg,[21] S. Grünendahl,[27]
G. Guglielmo,[50] J.A. Guida,[20] J.M. Guida,[51] A. Gupta,[11] S.N. Gurzhiev,[18] G. Gutierrez,[27]
P. Gutierrez,[50] N.J. Hadley,[38] H. Haggerty,[27] S. Hagopian,[25] V. Hagopian,[25] K.S. Hahn,[46]
R.E. Hall,[23] P. Hanlet,[40] S. Hansen,[27] J.M. Hauptman,[34] C. Hays,[44] C. Hebert,[35]
D. Hedin,[29] A.P. Heinson,[24] U. Heintz,[39] R. Hernández-Montoya,[14] T. Heuring,[25]
R. Hirosky,[28] J.D. Hobbs,[47] B. Hoeneisen,[6] J.S. Hoftun,[51] F. Hsieh,[41] Tong Hu,[31]
A.S. Ito,[27] J. Jaques,[32] S.A. Jerger,[42] R. Jesik,[31] T. Joffe-Minor,[30] K. Johns,[20]
M. Johnson,[27] A. Jonckheere,[27] M. Jones,[26] H. Jöstlein,[27] S.Y. Jun,[30] S. Kahn,[48]
D. Karmanov,[17] D. Karmgard,[25] R. Kehoe,[32] S.K. Kim,[13] B. Klima,[27] C. Klopfenstein,[22]
B. Knuteson,[21] W. Ko,[22] J.M. Kohli,[9] D. Koltick,[33] A.V. Kostritskiy,[18] J. Kotcher,[48]
A.V. Kotwal,[44] A.V. Kozelov,[18] E.A. Kozlovsky,[18] J. Krane,[34] M.R. Krishnaswamy,[11]
S. Krzywdzinski,[27] M. Kubantsev,[36] S. Kuleshov,[16] Y. Kulik,[47] S. Kunori,[38] F. Landry,[42]
G. Landsberg,[51] A. Leflat,[17] J. Li,[52] Q.Z. Li,[27] J.G.R. Lima,[3] D. Lincoln,[27] S.L. Linn,[25]
J. Linnemann,[42] R. Lipton,[27] J.G. Lu,[4] A. Lucotte,[47] L. Lueking,[27] A.K.A. Maciel,[29]
R.J. Madaras,[21] R. Madden,[25] L. Magaña-Mendoza,[14] V. Manankov,[17] S. Mani,[22]
H.S. Mao,[4] R. Markeloff,[29] T. Marshall,[31] M.I. Martin,[27] R.D. Martin,[28] K.M. Mauritz,[34]
B. May,[30] A.A. Mayorov,[18] R. McCarthy,[47] J. McDonald,[25] T. McKibben,[28] J. McKinley,[42]
T. McMahon,[49] H.L. Melanson,[27] M. Merkin,[17] K.W. Merritt,[27] C. Miao,[51] H. Miettinen,[54]
A. Mincer,[45] C.S. Mishra,[27] N. Mokhov,[27] N.K. Mondal,[11] H.E. Montgomery,[27]

1

M. Mostafa,[1] H. da Motta,[2] F. Nang,[20] M. Narain,[39] V.S. Narasimham,[11] A. Narayanan,[20] H.A. Neal,[41] J.P. Negret,[5] P. Nemethy,[45] D. Norman,[53] L. Oesch,[41] V. Oguri,[3] N. Oshima,[27] D. Owen,[42] P. Padley,[54] A. Para,[27] N. Parashar,[40] Y.M. Park,[12] R. Partridge,[51] N. Parua,[7] M. Paterno,[46] B. Pawlik,[15] J. Perkins,[52] M. Peters,[26] R. Piegaia,[1] H. Piekarz,[25] Y. Pischalnikov,[33] B.G. Pope,[42] H.B. Prosper,[25] S. Protopopescu,[48] J. Qian,[41] P.Z. Quintas,[27] R. Raja,[27] S. Rajagopalan,[48] O. Ramirez,[28] N.W. Reay,[36] S. Reucroft,[40] M. Rijssenbeek,[47] T. Rockwell,[42] M. Roco,[27] P. Rubinov,[30] R. Ruchti,[32] J. Rutherfoord,[20] A. Sánchez-Hernández,[14] A. Santoro,[2] L. Sawyer,[37] R.D. Schamberger,[47] H. Schellman,[30] J. Sculli,[45] E. Shabalina,[17] C. Shaffer,[25] H.C. Shankar,[11] R.K. Shivpuri,[10] D. Shpakov,[47] M. Shupe,[20] R.A. Sidwell,[36] H. Singh,[24] J.B. Singh,[9] V. Sirotenko,[29] P. Slattery,[46] E. Smith,[50] R.P. Smith,[27] R. Snihur,[30] G.R. Snow,[43] J. Snow,[49] S. Snyder,[48] J. Solomon,[28] X.F. Song,[4] M. Sosebee,[52] N. Sotnikova,[17] M. Souza,[2] N.R. Stanton,[36] G. Steinbrück,[50] R.W. Stephens,[52] M.L. Stevenson,[21] F. Stichelbaut,[48] D. Stoker,[23] V. Stolin,[16] D.A. Stoyanova,[18] M. Strauss,[50] K. Streets,[45] M. Strovink,[21] A. Sznajder,[3] P. Tamburello,[38] J. Tarazi,[23] M. Tartaglia,[27] T.L.T. Thomas,[30] J. Thompson,[38] D. Toback,[38] T.G. Trippe,[21] P.M. Tuts,[44] V. Vaniev,[18] N. Varelas,[28] E.W. Varnes,[21] A.A. Volkov,[18] A.P. Vorobiev,[18] H.D. Wahl,[25] J. Warchol,[32] G. Watts,[51] M. Wayne,[32] H. Weerts,[42] A. White,[52] J.T. White,[53] J.A. Wightman,[34] S. Willis,[29] S.J. Wimpenny,[24] J.V.D. Wirjawan,[53] J. Womersley,[27] D.R. Wood,[40] R. Yamada,[27] P. Yamin,[48] T. Yasuda,[27] P. Yepes,[54] K. Yip,[27] C. Yoshikawa,[26] S. Youssef,[25] J. Yu,[27] Y. Yu,[13] M. Zanabria,[5] Z. Zhou,[34] Z.H. Zhu,[46] M. Zielinski,[46] D. Zieminska,[31] A. Zieminski,[31] V. Zutshi,[46] E.G. Zverev,[17] and A. Zylberstejn[8]

(DØ Collaboration)

[1] Universidad de Buenos Aires, Buenos Aires, Argentina
[2] LAFEX, Centro Brasileiro de Pesquisas Físicas, Rio de Janeiro, Brazil
[3] Universidade do Estado do Rio de Janeiro, Rio de Janeiro, Brazil
[4] Institute of High Energy Physics, Beijing, People's Republic of China
[5] Universidad de los Andes, Bogotá, Colombia
[6] Universidad San Francisco de Quito, Quito, Ecuador
[7] Institut des Sciences Nucléaires, IN2P3-CNRS, Universite de Grenoble 1, Grenoble, France
[8] DAPNIA/Service de Physique des Particules, CEA, Saclay, France
[9] Panjab University, Chandigarh, India
[10] Delhi University, Delhi, India
[11] Tata Institute of Fundamental Research, Mumbai, India
[12] Kyungsung University, Pusan, Korea
[13] Seoul National University, Seoul, Korea
[14] CINVESTAV, Mexico City, Mexico
[15] Institute of Nuclear Physics, Kraków, Poland
[16] Institute for Theoretical and Experimental Physics, Moscow, Russia
[17] Moscow State University, Moscow, Russia
[18] Institute for High Energy Physics, Protvino, Russia
[19] Lancaster University, Lancaster, United Kingdom
[20] University of Arizona, Tucson, Arizona 85721
[21] Lawrence Berkeley National Laboratory and University of California, Berkeley, California 94720

^{22} *University of California, Davis, California 95616*

^{23} *University of California, Irvine, California 92697*

^{24} *University of California, Riverside, California 92521*

^{25} *Florida State University, Tallahassee, Florida 32306*

^{26} *University of Hawaii, Honolulu, Hawaii 96822*

^{27} *Fermi National Accelerator Laboratory, Batavia, Illinois 60510*

^{28} *University of Illinois at Chicago, Chicago, Illinois 60607*

^{29} *Northern Illinois University, DeKalb, Illinois 60115*

^{30} *Northwestern University, Evanston, Illinois 60208*

^{31} *Indiana University, Bloomington, Indiana 47405*

^{32} *University of Notre Dame, Notre Dame, Indiana 46556*

^{33} *Purdue University, West Lafayette, Indiana 47907*

^{34} *Iowa State University, Ames, Iowa 50011*

^{35} *University of Kansas, Lawrence, Kansas 66045*

^{36} *Kansas State University, Manhattan, Kansas 66506*

^{37} *Louisiana Tech University, Ruston, Louisiana 71272*

^{38} *University of Maryland, College Park, Maryland 20742*

^{39} *Boston University, Boston, Massachusetts 02215*

^{40} *Northeastern University, Boston, Massachusetts 02115*

^{41} *University of Michigan, Ann Arbor, Michigan 48109*

^{42} *Michigan State University, East Lansing, Michigan 48824*

^{43} *University of Nebraska, Lincoln, Nebraska 68588*

^{44} *Columbia University, New York, New York 10027*

^{45} *New York University, New York, New York 10003*

^{46} *University of Rochester, Rochester, New York 14627*

^{47} *State University of New York, Stony Brook, New York 11794*

^{48} *Brookhaven National Laboratory, Upton, New York 11973*

^{49} *Langston University, Langston, Oklahoma 73050*

^{50} *University of Oklahoma, Norman, Oklahoma 73019*

^{51} *Brown University, Providence, Rhode Island 02912*

^{52} *University of Texas, Arlington, Texas 76019*

^{53} *Texas A&M University, College Station, Texas 77843*

^{54} *Rice University, Houston, Texas 77005*

(August 6, 1999)

Abstract

We report the results of a study of color coherence effects in $p\overline{p}$ collisions based on data collected by the DØ detector during the 1994–1995 run of the Fermilab Tevatron Collider, at a center of mass energy $\sqrt{s} = 1.8$ TeV. Initial-to-final state color interference effects are studied by examining particle distribution patterns in events with a W boson and at least one jet. The data are compared to Monte Carlo simulations with different color coherence implementations and to an analytic modified-leading-logarithm perturbative calculation based on the local parton-hadron duality hypothesis.

3

Color coherence phenomena in the final state have been studied since the early 1980's in e^+e^- annihilations [1–6] and are very well established. The study of coherence effects in hadron–hadron collisions is considerably more subtle than those in e^+e^- annihilations due to the presence of colored constituents in both the initial and final states. In this paper we report the first results on initial-to-final state color interference effects in $p\overline{p}$ interactions using W+jets events.

Coherence phenomena are an intrinsic property of any gauge theory. In quantum chromodynamics (QCD), color coherence phenomena can be instructively separated into two regions: intrajet and interjet coherence [7,8]. Intrajet coherence deals with coherent effects in partonic cascades, resulting on average in the angular ordering (AO) of the sequential parton branches, which give rise to the depletion of soft particle production (the so called "hump-backed plateau") inside jets [9–11]. Interjet coherence is responsible for the string [12] or drag [13] effect first observed in the final state products of e^+e^- annihilations. It deals with the angular structure of soft particle flows when three or more energetic partons are involved in the hard process. In this case, the overall structure of particle angular distributions is governed by the underlying color dynamics of the hard scattering processes at short distances.

Perturbative quantum chromodynamics (pQCD) calculations have been used to describe the production of jet final states. However, descriptions of the characteristic particle structure of high energy hard collisions still rely on phenomenological models to explain how the partonic cascade evolves into final state hadrons. Within Monte Carlo (MC) simulations incorporating such models, the primary partons from the hard scatter evolve into jets of partons via gluon and quark emission according to pQCD. This process continues until a cut-off transverse-momentum scale ($Q_0 \approx 1$ GeV/c) is reached. After this phase, non-perturbative processes take over, which "cluster" the final partons into color singlet hadronic states via a mechanism described by phenomenological fragmentation models, like the Lund "string" [14] or the "cluster" [15] fragmentation models. These simulations usually involve many *a priori* unknown parameters that need to be tuned to the data.

A different and purely analytical approach giving quantitative predictions of hadronic spectra is based on the concept of Local Parton Hadron Duality (LPHD) [9]. The key assumption of this hypothesis is that the particle yield is described by a parton cascade in which the conversion of partons into hadrons occurs at a low virtuality scale, of the order of hadronic masses ($Q_0 \approx 200$ MeV/c^2) and independent of the scale of the primary hard process, and involves only low momentum transfers. It is assumed that the results obtained for partons apply to hadrons as well in an inclusive and average sense. Within the LPHD approach, resummed pQCD calculations for the parton cascade have been carried out in the simplest case (high energy limit) in the Double Logarithmic Approximation (DLA) [10,16], and in the Modified Leading Logarithmic Approximation (MLLA) [9,17,18], which includes higher order terms of relative order $\sqrt{\alpha_s}$ (e.g., finite energy corrections). These higher order terms are essential for quantitative agreement with data at present energies [7,19].

The AO approximation is an important consequence of color coherence. It results in the suppression of soft gluon radiation in partonic cascades in certain regions of phase space. For the case of outgoing partons, AO requires that the emission angles of soft gluons decrease monotonically as the partonic cascade evolves away from the hard process. MC simulations including coherence effects probabilistically by means of AO are available for both initial

and final state evolutions. (Parton shower event generators incorporate AO effects in the initial state as the time reversed process of the outgoing partonic cascade, i.e. the emission angles increase for the incoming partons as the process develops from the initial hadrons to the hard subprocess.) AO is an element of the DLA and MLLA analytic pQCD calculations, which provides the probabilistic interpretation of soft-gluon cascades. In fact, beyond the MLLA a probabilistic picture of the parton cascade evolution is not feasible due to $1/N_c^2$-suppressed (where N_c is the number of colors) soft interference contributions that appear in the higher-order calculations [8,17].

Both the CDF [20] and DØ [21] Collaborations have measured spatial correlations between the softer third jet and the second leading-E_T jet in $p\overline{p} \rightarrow 3\ jets + X$ events to explore the initial-to-final state coherence effects in $p\overline{p}$ interactions. The extraction of the color coherence signal in these measurements relies on comparisons of data distributions to MC simulations with and without coherence effects. In the analysis described here, the coherence signal in the data is extracted in a more direct way by comparing the soft particle angular distributions around the colorless W boson and opposing jet in the same event.

The DØ detector is described in detail elsewhere [22]. This analysis uses the tracking system and the uranium/liquid-argon sampling calorimeter. The DØ calorimeter has a transverse granularity of $\Delta\eta \times \Delta\phi = 0.1 \times 0.1$ forming projective towers, where η is the pseudorapidity ($\eta = -\ln[\tan(\theta/2)]$, θ is the polar angle with respect to the proton beam), and ϕ is the azimuthal angle. It has hermetic coverage for $|\eta| < 4.1$ with fractional transverse energy E_T resolution of $\approx 80\%/\sqrt{E_T(\text{GeV})}$ for jets and fractional energy resolution of $\approx 15\%/\sqrt{E(\text{GeV})}$ for electrons.

The data sample for this analysis [23], representing an integrated luminosity of 85 pb^{-1}, was collected during the 1994–1995 Tevatron Collider run. Events from $W \rightarrow e + \nu$ decays were collected with a trigger that required a minimum missing transverse energy ($\not{E}_T$) of 15 GeV and an isolated electromagnetic (EM) cluster with transverse energy $E_T > 20$ GeV. The offline kinematic requirements imposed on this sample were $\not{E}_T > 25$ GeV, $E_T^e > 25$ GeV, $|\eta_e| < 1.1$, and 40 GeV/c^2 $< M_T(e, \not{E}_T) < 110$ GeV/c^2, where $M_T(e, \not{E}_T) = \sqrt{2p_T(e)p_T(\nu)(1 - \cos\Delta\phi)/c^2}$ is the W boson transverse mass and $\Delta\phi$ is the azimuthal separation between the electron and neutrino. The transverse momentum of the neutrino, $p_T(\nu)$, was calculated using the calorimetric measurement of the $\not{E}_T$ in the event.

Events were required to have one electron cluster passing four quality criteria based on shower profile and tracking information: (i) the ratio of the EM energy to the total shower energy had to be greater than 0.95, (ii) the position of the calorimeter energy deposition of the electron had to match with a track found in the drift chambers, (iii) the lateral and longitudinal shape of the energy cluster had to be consistent with those of an electron, and (iv) the electron had to be isolated from other energy deposits in the calorimeter with isolation fraction $f_{\text{iso}} < 0.1$. The isolation fraction is defined as $f_{\text{iso}} = [E(0.4) - E_{\text{EM}}(0.2)]/E_{\text{EM}}(0.2)$, where $E(R_{\text{cone}})$ ($E_{\text{EM}}(R_{\text{cone}})$) is the total (electromagnetic) energy within a cone of radius $R_{\text{cone}} = \sqrt{(\Delta\eta)^2 + (\Delta\phi)^2}$ centered around the electron.

Jets in the events were reconstructed offline using an iterative fixed-cone clustering algorithm with cone radius $R_{\text{cone}} = 0.7$. Spurious jets from isolated noisy calorimeter cells and accelerator losses were eliminated by loose cuts on the jet shape.

5

Events were required to have a measured vertex with longitudinal position within 20 cm of the detector center to preserve the projective geometry. Since multiple interactions (more than one proton–antiproton interaction in the same bunch crossing) are expected to increase the global energy level in the calorimeter affecting the color coherence signal, we retained only events with a single reconstructed vertex and additionally required the beam-beam hodoscope timing information to be consistent with a single interaction. Finally, events were eliminated when there was significant pileup energy in the calorimeter around the region where the Tevatron Main Ring passes through the DØ detector.

We study color coherence in W+jets events by comparing the distributions of soft particles around the W boson and opposing leading-E_T jet. Since the W boson is a colorless object, it should not contribute to the production of secondary particles, thereby providing a template against which the pattern around the jet may be compared. This comparison reduces the sensitivity to global detector and underlying event biases that may be present in the vicinity of both the W boson and the jet.

The W boson was reconstructed from its electron and neutrino decay products, resulting in a twofold ambiguity in the W boson rapidity y_W (due to the corresponding ambiguity in the neutrino longitudinal momentum p_Z). MC studies have shown that the smaller $|y_W|$ is closer to the true W boson rapidity approximately 2/3 of the time, so this is the solution chosen. This choice was also made in the MC W boson reconstruction to retain consistency in the comparison with the data.

Once the W boson direction has been determined, the opposing jet was identified by selecting the leading-E_T jet in the azimuthal hemisphere opposite to the W boson. Annular regions are drawn around both the W boson and the tagged jet in (η, ϕ) space. The angular distributions of calorimeter towers with $E_T > 250$ MeV are measured in these annular regions using the polar variables $R = \sqrt{(\Delta\eta)^2 + (\Delta\phi)^2}$ and $\beta_X = \tan^{-1}(\frac{sign(\eta_X)\cdot\Delta\phi_X}{\Delta\eta_X})$; where $X = W$ or jet, $\Delta\eta_W = \eta_{\text{tower}} - y_W$, $\Delta\eta_{\text{jet}} = \eta_{\text{tower}} - \eta_{\text{jet}}$, and $\Delta\phi_X = \phi_{\text{tower}} - \phi_X$, in a search disk of $0.7 < R < 1.5$ (Fig. 1). For events in which the jet and the W boson annuli overlapped, all calorimeter towers in the shared region were assigned to the nearest object.

We define $\beta_{W(\text{jet})} = 0$ to point along the beam direction nearest to the W boson (jet). Calorimeter towers which correspond to partially instrumented calorimeter regions (regions between the central and end-cap calorimeter cryostats with pseudorapidities $1.1 < |\eta_{\text{tower}}| < 1.4$) were not included in the β distributions for either the data or MC simulations. Calorimeter cells that belong to the electron cluster in a cone of $R = 0.3$ from the centroid center were eliminated. We study the interference effects in regions $|\eta_{\text{jet}}| < 0.7$ and $|y_W| < 0.7$, requiring the tagged jet to have $E_T > 10$ GeV and the W boson $p_T > 10$ GeV/c. After application of all selection criteria 390 events remain.

The measured angular distributions are compared to the predictions of PYTHIA 5.7 [24] parton shower event generator with different levels of color coherence effects and to an analytic pQCD calculation of Khoze and Stirling [25] based on MLLA and LPHD. The PYTHIA MC sample was processed through a full GEANT-based detector simulation [26]. To best model the calorimeter noise effects in the MC simulations, we overlaid noise contributions for each calorimeter cell from the data. The generated events were subsequently processed using the same criteria employed for analyzing the data.

PYTHIA incorporates initial and final state color interference effects by means of the AO approximation of the parton cascades. After the perturbative phase it employs the Lund
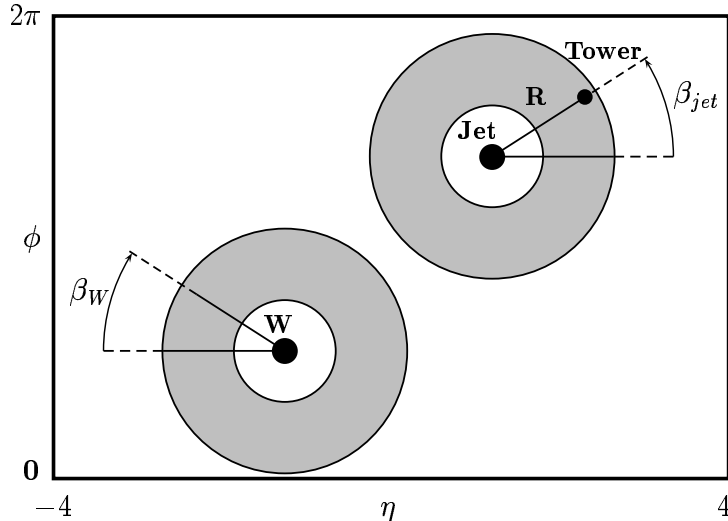
FIG. 1. Annular regions around the W boson and the tagged jet in (η, ϕ) space.

string fragmentation (SF) model (or an independent fragmentation IF model) as the phenomenological model to describe the non-perturbative hadronization process. The SF model has been supported by the observations of color coherence phenomena in e^+e^- annihilations. In PYTHIA, the AO constraint can be turned off. When both AO and SF are implemented, PYTHIA accounts for color coherence effects at both the perturbative and non-perturbative levels. Turning off AO removes the perturbative contribution, and using IF eliminates the non-perturbative component.

We check whether the MC simulations describe the event characteristics in the data using distributions of electron E_T, the event $\not{E}_T$, and the azimuthal and rapidity separation of the W boson and the tagged jet. These are compared to the PYTHIA simulations with full coherence effects in Fig. 2. For all distributions, PYTHIA is in good agreement with the data.

Figure 3(a) shows the measured angular distributions of the number of towers above threshold around the jet and around the W boson. The E_T of each calorimeter cell (each calorimeter tower is constructed from many calorimeter cells following the projective geometry of the detector with respect to the detector center) was corrected for offsets due to noise, zero suppression, and energy pileup effects [23]. A prominent feature of both curves is a strong peaking around $\pi/2 < \beta < 3\pi/4$. This is because the shapes of the β distributions are sensitive both to process dynamics and to phase space effects resulting from our event selection criteria and the calorimeter tower E_T threshold.

Figure 3(b) shows the ratio of the tower multiplicity around the jet to the tower multiplicity around the W boson as a function of β. The errors include only statistical uncertainties, which are the dominant source of uncertainty. The data show that the tower multiplicity around the jet is greater than that around the W boson and the excess is enhanced in the event plane (i.e., the plane defined by the directions of the W boson or jet and the beam axis: $\beta = 0, \pi$) and minimized in the transverse plane ($\beta = \pi/2$). This is consistent with the expectation from initial-to-final state color interference that there is an enhancement of soft
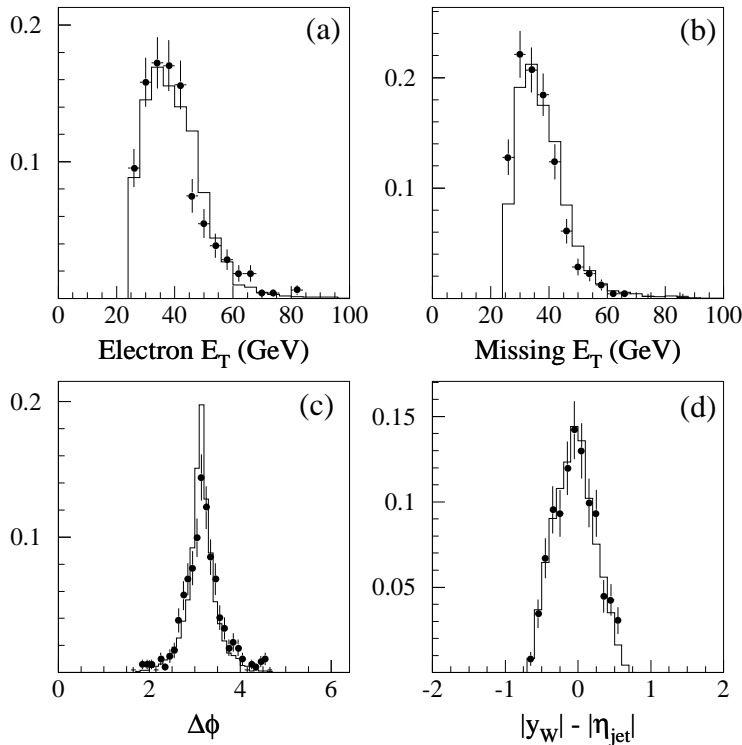
7

FIG. 2. Comparisons of data (points) with PYTHIA events with AO and SF (histogram) for (a) electron E_T, (b) event $\not{E}_T$, (c) azimuthal separation of the W boson and tagged jet, and (d) rapidity separation of the W boson and tagged jet.

particle production around the tagged jet in the event plane relative to the transverse plane when compared with the particle production around the W boson. It is also in agreement with our published multijet analysis results [21].

The ratio of the tower multiplicity around the jet to the tower multiplicity around the W boson is shown in Fig 4 for the data and the MC predictions as a function of β. All predictions have been normalized to the integral of the data β-distribution. PYTHIA with AO and SF is in good agreement with the W+jets data. PYTHIA with AO off and SF agrees less well, and PYTHIA with AO off and IF does not reproduce the data. The shape of the analytic prediction based on MLLA and LPHD is consistent with the data as shown in Fig. 4(d). We note that the analytic calculation was performed assuming that the W boson and the outgoing parton were produced centrally and does not include any underlying event or detector simulation effects.

To measure the color coherence signal, we construct the variable $R_{\rm sig}$ as the jet/W boson tower multiplicity ratio of the event plane $(\beta = 0, \pi)$ to the transverse plane $(\beta = \pi/2)$. We define $R_{\rm sig} = \frac{R(\beta=0,\pi)}{R(\beta=\pi/2)}$, where $R(\beta = 0, \pi) = \frac{N_{\rm jet}^{1^{st}bin}+N_{\rm jet}^{7^{th}bin}}{N_W^{1^{st}bin}+N_W^{7^{th}bin}}$, $R(\beta = \pi/2) = \frac{N_{\rm jet}^{4^{th}bin}}{N_W^{4^{th}bin}}$, and $N_{W({\rm jet})}^{i^{th}bin}$ is the number of towers above threshold for the ith bin of the W boson (jet) β distribution. $R_{\rm sig}$ is expected to be near unity in the absence of color coherence effects. In addition $R_{\rm sig}$ is insensitive to the overall normalization of the individual distributions,
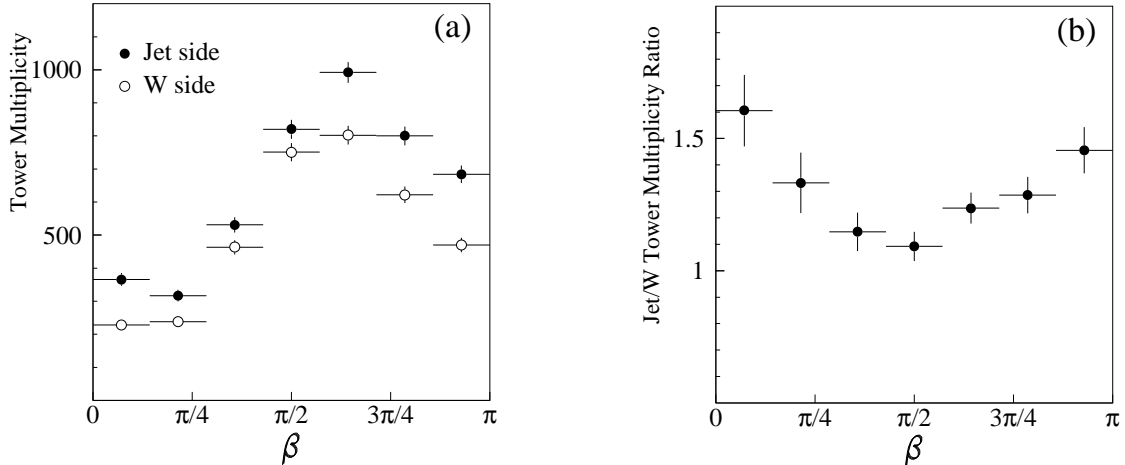
FIG. 3. (a) Calorimeter tower multiplicity around the jet and W boson as a function of β. (b) Ratio of the tower multiplicity around the jet to the tower multiplicity around the W boson as a function of β.

and MC studies have shown that it is relatively insensitive to detector smearing effects. Figure 5 compares the R_{sig} variable for the data to the various PYTHIA predictions and to the MLLA+LPHD calculation. Clearly the value of R_{sig} for the data deviates from unity in agreement with PYTHIA with AO on and SF, and in disagreement with AO off and SF or AO off and IF. These comparisons imply that for the process under study, string fragmentation alone cannot describe the effects seen in the data. The AO approximation is an element of parton-shower event generators that needs to be included if color coherence effects are to be modeled successfully. Finally, the analytic prediction by Khoze and Stirling is consistent with the data, thus giving additional evidence supporting the validity of the LPHD hypothesis.

The dominant source of uncertainty on the data β distributions is statistical due to the limited event sample. The statistical error for R_{sig} is 7%. Since we report ratios of event distributions any possible uncertainty on quantities that affect the overall rate of events is minimized. Sources of systematic uncertainty arise from background contamination to W+jets events, uncertainties in the calorimeter channel-to-channel offset correction, multiple $p\bar{p}$ interactions, and uncertainties associated with the calorimeter tower E_T threshold. The primary background to W+jets events is dijet production in which one of the jets mimics the characteristics of an electron. The $\not{E}_T$ in such events typically arises from shower fluctuations or calorimeter imperfections. For our selection criteria, the estimated background level is about 5% resulting in a 1-2% uncertainty on the coherence signal. The effect on the R_{sig} variable due to uncertainties in the offset correction were found to be at the 1% level. To evaluate possible effects on the signal coming from residual multiple interaction contamination, we examined the dependence of R_{sig} as a function of luminosity. No systematic dependence of the signal variable was observed for our event sample.

The dependence of the signal variable R_{sig} on the calorimeter tower E_T threshold was studied by varying the threshold from 200 to 350 MeV. Figure 6 shows how the R_{sig} variable
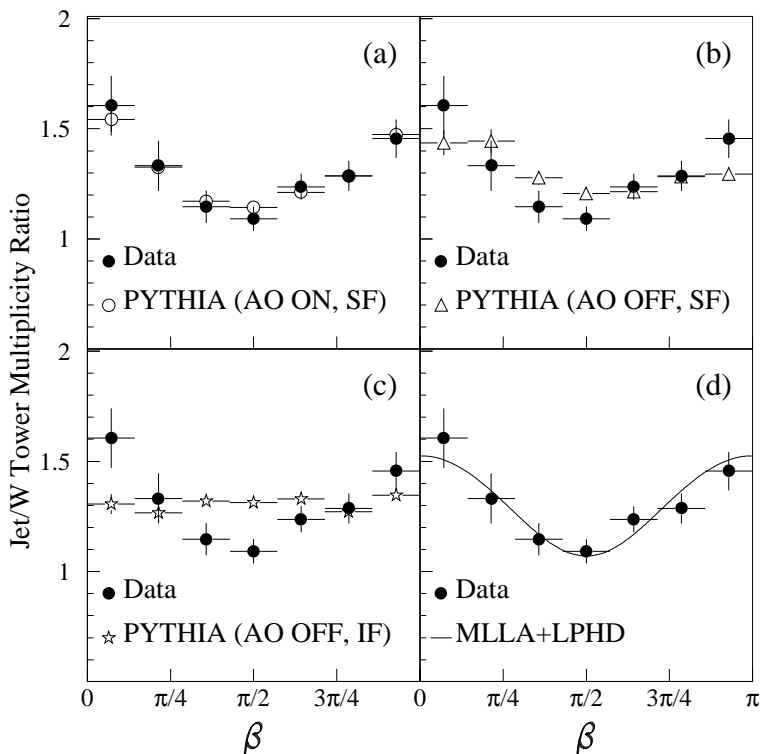
9

FIG. 4. Comparison of the Jet/W boson tower multiplicity ratio from data to (a) PYTHIA with AO on and SF, (b) AO off and SF, (c) AO off and IF, and to the (d) MLLA+LPHD predictions. The predictions have been normalized to the data. All uncertainties are statistical only.

varies as a function of the tower threshold for the data and for the three PYTHIA predictions. Although there seems to be a dependence of R_{sig} with the tower E_T threshold for both the data and the simulations, for all tower thresholds examined the PYTHIA predictions with AO on and with SF resemble the data best.

In summary, color coherence effects in $p\overline{p}$ interactions have been observed and studied by the DØ Collaboration. We have presented the first results on color coherence effects in W+jets events. The data show an enhancement of soft particle radiation around the jet in the event plane with respect to the transverse plane, consistent with color coherence as implemented in the PYTHIA parton shower event generator, which includes the angular ordering approximation and string fragmentation. In addition, the relative amount of enhancement is consistent with an analytic perturbative QCD calculation based on modified leading logarithmic approximation and local parton-hadron duality.
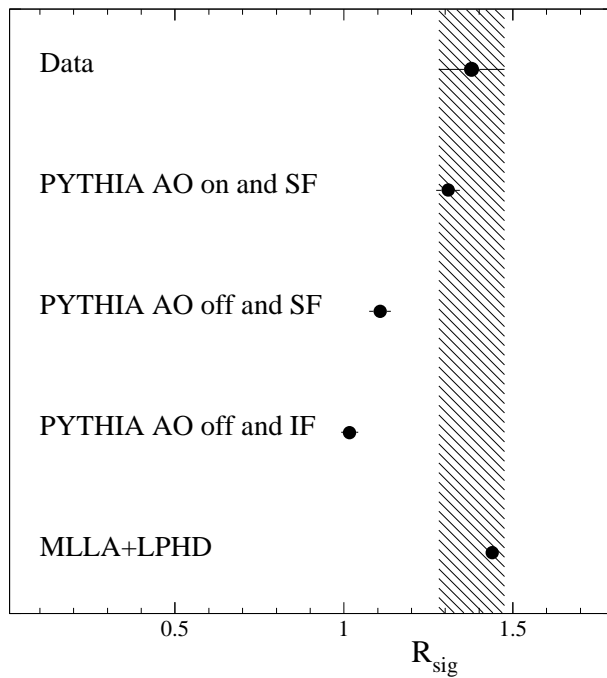
FIG. 5. R_{sig} for DØ data, PYTHIA with various coherence implementations, and a MLLA+LPHD QCD calculation. The errors are statistical only and the shaded band shows the statistical uncertainty on the R_{sig} variable for the data.
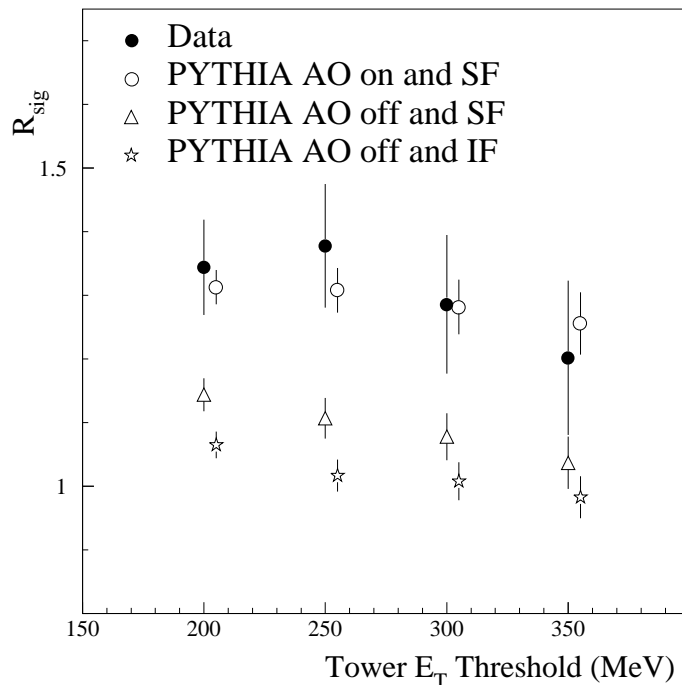
FIG. 6. $R_{\rm sig}$ as a function of the tower E_T threshold for the data (solid circles) and for the various PYTHIA predictions. All uncertainties are statistical only.

REFERENCES

[1] JADE Collaboration, W. Bartel *et al.*, Phys. Lett. B **101**, 129 (1981); Z. Phys. **C21**, 37 (1983); Phys. Lett. B **134**, 275 (1984); Phys. Lett. B **157**, 340 (1985).

[2] TPC/2γ Collaboration, H. Aihara *et al.*, Phys. Rev. Lett. **54**, 270 (1985); Z. Phys. **C28**, 31 (1985); Phys. Rev. Lett. **57**, 945 (1986).

[3] TASSO Collaboration, M. Althoff *et al.*, Z. Phys. **C29**, 29 (1985).

[4] MARK II Collaboration, P.D. Sheldon *et al.*, Phys. Rev. Lett. **57**, 1398 (1986).

[5] OPAL Collaboration, M.Z. Akrawy *et al.*, Phys. Lett. B **247**, 617 (1990); Phys. Lett. B **261**, 334 (1991); P.D. Acton *et al.*, Phys. Lett. B **287**, 401 (1992); Z. Phys. **C58**, 207 (1993).

[6] L3 Collaboration, M. Acciarri *et al.*, Phys. Lett. B **353**, 145 (1995).

[7] For a recent discussion of the phenomenological status and comparisons to data, see V.A. Khoze and W. Ochs, Int. J. Mod. Phys. **A12**, 2949 (1997).

[8] Yu.L. Dokshitzer, V.A. Khoze, A.H. Mueller, and S.I. Troyan, "Basics of Perturbative QCD" (Editions Frontières, Gif-sur-Yvette, 1991).

[9] Ya.I. Azimov, Yu.L. Dokshitzer, V.A. Khoze, and S.I. Troyan, Z. Phys. **C27**, 65 (1985) and **C31**, 213 (1986).

[10] Yu.L. Dokshitzer, V.S. Fadin, and V.A. Khoze, Phys. Lett. B **115**, 242 (1982); Z. Phys. **C15**, 325 (1982).

[11] A. Bassetto, M. Ciafaloni, G. Marchesini, and A.H. Mueller, Nucl. Phys. **B207**, 242 (1982).

12

[12] B. Andersson, G. Gustafson, and T. Sjöstrand, Phys. Lett. B **94**, 211 (1980).

[13] Ya.I. Azimov, Yu.L. Dokshitzer, V.A. Khoze, and S.I. Troyan, Phys. Lett. B **165**, 147 (1985); Sov. Journ. Nucl. Phys. **43**, 95 (1986).

[14] B. Andersson, G. Gustafson, G. Ingelman, and T. Sjöstrand, Phys. Rep. **97**, 31 (1983).

[15] G. Marchesini *et al.*, Computer Physics Commun. **67**, 465 (1992).

[16] A. Bassetto, M. Ciafaloni, and G. Marchesini, Phys. Rep. **C100**, 201 (1983).

[17] Yu.L. Dokshitzer and S.I. Troyan, in *Proceedings of the 19th Winter School of the LNPI*, Vol. 1, p.144 (Leningrad preprint LNPI-922, 1984).

[18] A.H. Mueller, Nucl. Phys. **B213**, 85 (1983); Erratum quoted ibid. **B241**, 141 (1984).

[19] N. Varelas, in *Proceedings of the XVIII Physics in Collision Conference, Frascati, Italy*, edited by S. Bianco, A. Calcaterra, P. de Simone, F.L. Fabbri, (INFN Laboratory, Frascati, 1998), p.107 (hep-ex/9809019).

[20] CDF Collaboration, F. Abe *et al.*, Phys. Rev. D **50**, 5562 (1994).

[21] DØ Collaboration, B. Abbott *et al.*, Phys. Lett. B **414**, 419 (1997).

[22] DØ Collaboration, S. Abachi *et al.*, Nucl. Instrum. Meth. **A338**, 185 (1994).

[23] J. Jaques, Ph.D. Dissertation, University of Notre Dame, 1996, (unpublished), *http://www-d0.fnal.gov/results/publications_talks/thesis/thesis.html*.

[24] T. Sjöstrand, Computer Physics Commun. **82**, 74 (1994).

[25] V.A. Khoze and J. Stirling, Z. Phys. **C76**, 59 (1997).

[26] R. Brun *et al.*, "GEANT 3.14", CERN, DD/EE/84-1, (unpublished).